Micromechanical study of the loading path effect in high cycle fatigue

R. Guerchais[a,b,*], C. Robert[a], F. Morel[a], N. Saintier[b]

[a] *Arts et Metiers ParisTech, LAMPA, 2 bd du Ronceray, 49035 Angers Cedex, France*
[b] *Arts et Metiers ParisTech, I2M - UMR CNRS 5295, Université Bordeaux 1, Esplanade des Arts et Métiers, 33405 Talence Cedex, France*

Abstract

In this work, an analysis of both the mechanical response at the grain scale and high cycle multiaxial fatigue criteria is undertaken using finite element (FE) simulations of polycrystalline aggregates. The metallic material chosen for investigation, a pure copper, has a Face Centred Cubic (FCC) crystalline structure. Two-dimensional polycrystalline aggregates, which are composed of 300 randomly orientated equiaxed grains, are loaded at the median fatigue strength defined at 10^7 cycles. In order to analyse the effect of the loading path on the local mechanical response, combined tension-torsion and biaxial tension loading cases, in-phase and out-of-phase, with different biaxiality ratios, are applied to each polycrystalline aggregate. Three different material constitutive models assigned to the grains are investigated: isotropic elasticity, cubic elasticity and crystal plasticity in addition to the cubic elasticity. First, some aspects of the mechanical response of the grains are highlighted, namely the scatter and the multiaxiality of the mesoscopic responses with respect to an uniaxial macroscopic response. Then, the distributions of relevant mechanical quantities classically used in fatigue criteria are analysed for some loading cases and the role of each source of anisotropy on the mechanical response is evaluated and compared to the isotropic elastic case. In particular, the significant influence of the elastic anisotropy on the mesoscopic mechanical response is highlighted. Finally, an analysis of three different fatigue criteria is conducted, using mechanical quantities computed at the grain scale. More precisely, the predictions provided by these criteria, for each constitutive model studied, are compared with

*Corresponding author. Tel: +33 (0)2 41 20 73 27; fax: +33 (0)2 41 20 73 20
Email address: raphael.guerchais@ensam.eu (R. Guerchais)

the experimental trends observed in metallic materials for such loading conditions.

Keywords: Multiaxial high cycle fatigue, Microstructure modeling, Anisotropic elasticity, Crystal plasticity, Fatigue criterion

---

Nomenclature

γ_s : plastic slip on the slip system s

ν_s : accumulated plastic slip on the slip system s

τ_s : resolved shear stress on the slip system s

r_s : isotropic hardening variable on the slip system s

x_s : kinematic hardening variable on the slip system s

$\boldsymbol{\sigma}$: stress tensor

$\boldsymbol{\varepsilon}^p$: plastic strain tensor

$\underline{n}_s$: unit vector normal to the slip plane (Fig.1)

$\underline{l}_s$: unit vector in the slip direction (Fig.1a)

$\boldsymbol{m}_s$: orientation tensor of the slip system s

$\langle \bullet \rangle_a$: volume-weighted average over the aggregate

$\langle \bullet \rangle_g$: volume-weighted average over the grain g

$\boldsymbol{\Sigma} = \langle \boldsymbol{\sigma} \rangle_a$: macroscopic stress tensor

$\langle \boldsymbol{\sigma} \rangle_g$: mesoscopic stress tensor

$\underline{\sigma}(\underline{n})$: mesoscopic stress vector across the plane of unit normal vector $\underline{n}$ (Fig.1b)

$\underline{\tau}$: mesoscopic shear stress vector (Fig.1b)

τ_a : mesoscopic shear stress amplitude (Fig.1b)

τ_m : mesoscopic mean shear stress (Fig.1b)

$T_{s,a}$: macroscopic resolved shear stress amplitude on the slip system s

$\tau_{s,a}$: mesoscopic resolved shear stress amplitude on the slip system s (Fig.1b)

Σ_n : macroscopic normal stress acting on the plane $\underline{n}$

σ_n : mesoscopic normal stress acting on the plane $\underline{n}$ (Fig.1b)

$\sigma_{n,a}$: mesoscopic normal stress amplitude acting on the plane $\underline{n}$

$\sigma_{n,m}$: mesoscopic mean normal stress acting on the plane $\underline{n}$

σ_h : mesoscopic hydrostatic stress

P_{Fn} : failure probability of a slip plane

P_{Fg} : failure probability of a grain

P_{Fa} : failure probability of an aggregate

1. Introduction

Fatigue crack initiation in metallic materials is a local phenomenon intimately related to the plastic activity at the grain scale. Indeed, in High Cycle Fatigue (HCF), it has been observed that the plastic deformation localises heterogeneously in some favourably-oriented grains leading to slip bands formation and to fatigue cracks initiation mainly at the interface between these bands and the surrounding matrix. In this context, it seems relevant to try to evaluate the mesoscopic mechanical quantities (i.e. the average values per grain) in order to study the HCF strength. Unfortunately, due to complex anisotropic elasto-plastic behaviour of the crystals constituting a metal, no simple method exists to precisely estimate these quantities.

Homogenisation schemes are a common way to relate the mechanical response of each grain to the macroscopic loading applied to a polycrystal. This approach has been successfully used in the development of HCF criteria. The first attempt of multiscale approach in fatigue was proposed by Dang Van [1]. The work of Papadopoulos [2], a continuation of the one of Dang Van, has allowed improvements such as a better consideration of the effect of phase shift on the fatigue strength of metals under combined tension and torsion. Monchiet et al. [3] have developed a criterion based, like the one proposed by Dang Van, on the elastic shakedown concept but in which the damage is coupled to plasticity in order to explain the mean stress effect in HCF. Morel et al. [4], starting from the definition of the fatigue crack initiation criterion at the grain scale proposed by Papadopoulos, has constructed a criterion in a probabilistic framework allowing to take into account the variability of the fatigue crack initiation threshold and providing satisfactory predictions for biaxial loading cases (combined tension and torsion, biaxial tension) [5]. Despite the qualities of these criteria (ease of application, fairly accurate predictions), simplifying assumptions are made in their development. The influence of these hypotheses (for instance, the consideration that the elastic behaviour is the same at the grain scale and at the macroscopic scale) on the predictions is not necessarily quantified. Moreover neighbouring and free surface effects can hardly be taken into

account.

A promising approach, consisting in computing, by FE method, the mechanical response of explicitly modelled polycrystalline aggregates, allows to take into account microstructural details generally neglected in the homogenisation schemes and to deepen the analysis of the mesoscopic mechanical responses of metals under cyclic multiaxial loading. In recent years, several works have involved this kind of numerical simulations to contribute to the study of the HCF behaviour. For instance, Benett et al. [6] have analysed the distribution of fatigue crack initiation parameters inspired from well-known HCF criteria. This study was enriched by the work of Guilhem et al. [7] in which the mechanical response of the grains is studied according to their position in the aggregate (for instance at the free surface or in the core), their orientation and the one of the neighbouring grains. Moreover, a study of Robert et al. [8] has highlighted the important role played by the cubic elasticity in the mesoscopic responses of polycrystalline copper. At last, others factors affecting fatigue strength, such as surface roughness or pre-hardening, began to be investigated [9],[10].

The present study falls within this framework and is divided into two parts:

- The first part consists in an investigation of the role of each source of anisotropy (i.e. elastic and plastic) on the mesoscopic mechanical responses of a polycrystalline copper cyclically loaded, at levels corresponding to the median fatigue limit at 10^7 cycles, in various biaxial loading conditions ;
- The second part is dedicated to the evaluation of the predictions of three fatigue criteria, inspired by those proposed by Dang Van [1], Papadopoulos [2] and Morel and Huyen [4], using the results of the FE simulations in the cases of combined tension-shear and biaxial tension and a comparison of these predicted fatigue limits with experimental trends.

2. Modelling approach

2.1. Constitutive material models at the grain scale

The anisotropic behaviour of the grains is due, on the one hand, to the elastic behaviour and, on the other hand, to the crystallographic nature of the plastic slip. In FCC structure, as for pure copper, the elastic behaviour is cubic and the plastic slip occurs along the {111}

planes in the $\langle 110 \rangle$ directions which correspond respectively to the closed-packed planes and directions of this crystal structure. In order to dissociate the effect of each sources of anisotropy on the mesoscopic mechanical responses, three constitutive models, assigned to the grains, are investigated:

- Linear isotropic elasticity;
- Linear cubic elasticity;
- Linear cubic elasticity with crystal plasticity.

In each case, a Hooke's law is used to describe the elastic behaviour. In the first case, an isotropic elastic behaviour is considered and is defined by the Young's Modulus E and the Poisson's ratio ν. In the second and third cases, cubic elasticity is considered and completely characterised by three coefficients defined in the crystal coordinate system : C_{1111}, C_{1122} and C_{1212}.

Finally, crystal plasticity is described by a single crystal visco-plastic model proposed by Méric et al. [11]. In this constitutive model, the plastic slip rate $\dot{\gamma}_s$ on a slip system s is governed by a Norton-type flow rule (Eq. 1) involving the resolved shear stress τ_s acting on s and the isotropic and kinematic hardening variables, resp. r_s and x_s, associated to s.

$$\dot{\gamma}_s = \left\langle \frac{|\tau_s - x_s| - r_0 - r_s}{K} \right\rangle_+^n sgn(\tau_s - x_s) = \dot{\nu}_s sgn(\tau_s - x_s) \tag{1}$$

where K and n are the parameters defining the viscosity and r_0 corresponds to the critical resolved shear stress. The resolved shear stress τ_s acting on s is computed from the stress tensor $\boldsymbol{\sigma}$ by means of the orientation tensor $\boldsymbol{m}_s$ (Eqs 2 and 3). This tensor allows also to compute the plastic strain rate tensor $\dot{\boldsymbol{\varepsilon}}^p$ knowing the plastic slip rate $\dot{\gamma}_s$ occurring on each slip system s (Eq. 4).

$$\tau_s = \boldsymbol{m}_s : \boldsymbol{\sigma} \tag{2}$$

$$\boldsymbol{m}_s = \frac{(\underline{n}_s \otimes \underline{l}_s + \underline{l}_s \otimes \underline{n}_s)}{2} \tag{3}$$

$$\dot{\boldsymbol{\varepsilon}}^p = \sum_s \dot{\gamma}_s \boldsymbol{m}_s \tag{4}$$

The evolution laws of the hardening variables r_s and x_s are respectively given by Eqs 5 and 6.

$$r_s = Q \sum_r h_{sr} (1 - e^{-b\nu_r}) \tag{5}$$

Isotropic elasticity		Cubic elasticity		
E [GPa]	ν	C_{1111} [GPa]	C_{1122} [GPa]	C_{1212} [GPa]
118	0.344	159	122	81

Viscosity		Kinematic hardening	
K [MPa.s$^{1/n}$]	n	c [MPa]	d
8	20	32000	900

Isotropic hardening								
r_0 [MPa]	Q [MPa]	b	h_0	h_1	h_2	h_3	h_4	h_5
15	4	12	1	1	0.2	90	3	2.5

Table 1: Material parameters.

$$\dot{x}_s = c\dot{\gamma}_s - d\dot{\nu}_s x_s \tag{6}$$

In Eq. 5, the influence of the accumulated plastic slip ν_r on the slip system r on the hardening of the slip system s is taken into account thanks to the components h_{sr} of the interaction matrix, introduced by Franciosi [12]. Q and b are the other isotropic hardening parameters and c and d are the kinematic hardening parameters (Eq. 6).

The material parameters values used in the FE simulation, identified by Méric et al. [11] and Gérard et al. [13], are summarised in Table 1.

2.2. Finite element modelling

The process used to generate periodic 2-dimensional polycrystalline aggregates geometries is described in [8]. The finite element mesh of the CAD of the synthetic microstructure, containing 300 equiaxed grains, is obtained using Gmsh [14]. Three-nodes triangular finite elements, with linear interpolation and generalised plane strain hypothesis, are used. The grains are discretised in average with 100 elements. An illustration of a geometry and a finite element mesh of a microstructure is shown in Fig.2.

For each loading condition and constitutive model studied, three different microstructure geometries and three different orientation sets are used. Each orientation set are composed by 300 triplets of Euler angles chosen such as to represent an isotropic crystallographic texture. Each triplet of Euler angles defines the orientation of one crystal frame with respect to the reference frame of the aggregate. As a result, the mechanical response of nine different

microstructures is investigated per loading condition and per constitutive model.

Thanks to the linearity of the elastic behaviours, only one loading cycle is computed when purely elastic constitutive models are assigned to the grains. In the case where crystal plasticity is used, 10 loading cycles are applied so that the aggregates tend to a stabilised behaviour at the local scale. Periodic displacement boundary conditions are imposed at the edge of the polycrystalline aggregates. Computations are performed by imposing the macroscopic stress tensor $\mathbf{\Sigma}$, i.e. the volume-weighted average of the stress tensors over the entire aggregate, as it is usually the case when characterising the HCF behaviour experimentally.

The numerical simulations are conducted with the ZéBuLoN FE software developped by Mines ParisTech, NorthWest Numerics and ONERA [15].

2.3. Loading conditions

Two types of loading conditions are applied to the polycrystalline aggregates in this work: combined tension and shear, representative of the stress state encountered in tension-torsion fatigue test, and biaxial tension. The corresponding applied macroscopic stress tensors are respectively expressed, in the aggregate coordinate system, by Eqs 7 and 8.

$$\text{Tension-shear: } \mathbf{\Sigma} = \begin{bmatrix} \Sigma_{11,a}\sin(\omega t) & \Sigma_{12,a}\sin(\omega t - \varphi_{12}) & 0 \\ \Sigma_{12,a}\sin(\omega t - \varphi_{12}) & 0 & 0 \\ 0 & 0 & 0 \end{bmatrix}_{(\underline{e_1},\underline{e_2},\underline{e_3})} \tag{7}$$

$$\text{Biaxial tension: } \mathbf{\Sigma} = \begin{bmatrix} \Sigma_{11,a}\sin(\omega t) & 0 & 0 \\ 0 & \Sigma_{22,a}\sin(\omega t - \varphi_{22}) & 0 \\ 0 & 0 & 0 \end{bmatrix}_{(\underline{e_1},\underline{e_2},\underline{e_3})} \tag{8}$$

The choice of these loading conditions is motivated by the fact that, on the one hand, some of them deviate in terms of stress state from usual loading cases used to identify the fatigue criteria, especially the biaxial tension, and on the other hand, results of fatigue tests on metallic materials are reported in the literature for these kinds of loading [5, 16–21]. Several biaxiality ratios (k_{12} and k_{22}) and phase shifts (φ_{12} and φ_{22}) have been selected for this work (Tables 2 and 3). Each of these loading cases are studied when purely elastic models are assigned to the grains but only a few of them are analysed when crystal plasticity is used because of the high computation time induced by the use of such a constitutive model.

$k_{12} = \Sigma_{12,a}/\Sigma_{11,a}$							φ_{12} [°]				
0	0.25	0.5	0.75	1	2	∞	0	30	45	60	90

Table 2: Biaxiality ratios k_{12} and phase shifts φ_{12} studied for the combined tension and shear loading cases

$k_{22} = \Sigma_{22,a}/\Sigma_{11,a}$					φ_{22} [°]								
0	0.25	0.5	0.75	1	0	30	45	60	90	120	135	150	180

Table 3: Biaxiality ratios k_{22} and phase shifts φ_{22} studied for the biaxial tension loading cases

3. Fatigue criteria

The predictions of three different fatigue criteria are studied in this work. Their expressions derive from multiaxial HCF fatigue criteria based on the mesoscopic approaches proposed by Dang Van [1], Papadopoulos [2] and Morel and Huyen [4]. The main change made on these criteria is the replacement of the macroscopic mechanical quantities by mesoscopic mechanical quantities, i.e. the quantities computed from the stress tensors averaged per grain $\langle \boldsymbol{\sigma} \rangle_g$ which are obtained from the last loading cycle of the FE simulations.

3.1. Critical plane-based criterion

The criterion proposed by Dang Van is based on the assumption that the fatigue crack initiation in one grain leads to the failure of the entire polycrystalline aggregate. To keep this idea, a criterion checking that no crack initiates during the last loading cycle in each slip plane contained in the polycrystal is proposed (Eq. 9). With this relation, which is similar to the one proposed by Dang Van, it is assumed that the fatigue failure is prevented as long as the inequality is satisfied.

$$\sigma_{DV} = \max_{\underline{n}} \left[\max_{t} \left[\| \underline{\tau}(\underline{n}, t) - \underline{\tau}_m(\underline{n}) \| + \alpha_{DV} \sigma_h(t) \right] \right] \leq \beta_{DV} \tag{9}$$

α_{DV} and β_{DV} are two material parameters. $\underline{\tau}(\underline{n}, t)$ represents the mesoscopic shear stress vector acting on the slip plane $\underline{n}$, $\underline{\tau}_m(\underline{n})$ the mesoscopic mean shear stress vector acting on the

slip plane $\underline{n}$ and $\sigma_h(t)$ the mesoscopic hydrostatic pressure. As the direction of the mesoscopic shear stress vector $\underline{\tau}(\underline{n},t)$ generally changes with time, the end of this vector described a path Γ (Fig.1b) during the last loading cycle. Under these conditions, an appropriate definition of the mesoscopic mean shear stress vector $\underline{\tau}_m(\underline{n})$, to respect its uniqueness [22], consist to define $\underline{\tau}_m(\underline{n})$ as the vector $\underline{O\Omega}$ with O being the origin of the shear stress vector and Ω being the centre of the smallest circle circumscribing the path Γ (Fig.1b). The randomised algorithm summarised in [22] is used to efficiently find the minimum enclosing circle of the path of each slip plane.

3.2. Papadopoulos criterion

Like Dang Van, Papadopoulos has developed a fatigue criterion at the grain scale based on the concept of elastic shakedown. In this mesoscopic fatigue criterion, a fatigue crack does not initiate in a grain if the accumulated plastic slip on its slip systems does not exceed a threshold.

Papadopoulos wisely noticed that the engineering fatigue limit is not considered as the stress amplitude at which there is no crack initiation. The author relies on the fact that non-propagating small fatigue cracks can be observed in specimens loaded below their conventional fatigue limit. This leads Papadopoulos to propose a criterion, given in Eq.10, based on an estimate of the average accumulated plastic slip of all the slip systems contained in a representative volume element (RVE). This criterion is expressed in function of the quadratic mean, along every slip systems in the polycrystal, of the macroscopic resolved shear stress amplitude $T_{s,a}$ (Eq. 11) and the average, along every slip planes in the polycrystal, of the macroscopic normal stess Σ_n (Eq. 12).

$$\sqrt{\langle T_{s,a}^2 \rangle} + \alpha \max_t \left[\langle \Sigma_n(t) \rangle \right] \leq \beta \tag{10}$$

$$\sqrt{\langle T_{s,a}^2 \rangle} = \sqrt{5} \sqrt{\frac{1}{8\pi^2} \int_{\varphi=0}^{2\pi} \int_{\theta=0}^{\pi} \int_{\chi=0}^{2\pi} T_{s,a}^2 d\chi \sin(\theta) d\theta d\varphi} \tag{11}$$

$$\langle \Sigma_n(t) \rangle = \frac{1}{8\pi^2} \int_{\varphi=0}^{2\pi} \int_{\theta=0}^{\pi} \int_{\chi=0}^{2\pi} \Sigma_n(t) d\chi \sin(\theta) d\theta d\varphi \tag{12}$$

In this work, the form of this criterion is preserved (Eq. 13) but mesoscopic quantities are used instead of the macroscopic ones ($\tau_{s,a}$ and σ_n replace respectively $T_{s,a}$ and Σ_n):

$$\sigma_P = \sqrt{\langle \tau_{s,a}^2 \rangle} + \alpha_P \max_t \left[\langle \sigma_n(t) \rangle \right] \leq \beta_P \tag{13}$$

where α_P and β_P correspond to the material parameters. As the microstructures studied contain a finite number of grains and slip systems, $\sqrt{\langle \tau_{s,a}^2 \rangle}$ and $\langle \sigma_n \rangle$ become

$$\sqrt{\langle \tau_{s,a}^2 \rangle} = \sqrt{5} \sqrt{\frac{1}{N_s} \sum_{g=1}^{N_g} \left[f(g) \sum_{s=1}^{N_s} \tau_{s,a}^2(g,s) \right]} \tag{14}$$

$$\langle \sigma_n(t) \rangle = \frac{1}{N_p} \sum_{g=1}^{N_g} \left[f(g) \sum_{p=1}^{N_p} \sigma_n(g,p,t) \right] \tag{15}$$

where N_s and N_p are respectively the number of slip systems in a grain and the number of slip planes in a grain. In Eqs 14 and 15, $f(g)$ represents the volume fraction of the grain g. For the sake of simplicity, as the grains in the microstructure have approximately the same volume, $f(g)$ is assumed to be equal to $1/N_g$ with N_g being the number of grains in the considered microstructure.

3.3. Probabilistic fatigue criterion

Morel and Huyen have proposed a criterion based on the assumption that the fatigue crack initiation threshold at the grain scale follows a Weibull distribution which led them to define a failure probability for each grain contained in a polycrystalline aggregate. In order to estimate the failure probability of the polycrystal, the authors then applied the weakest-link hypothesis. This reasoning is repeated below.

First, a fatigue crack is assumed to initiate in a slip plane of normal $\underline{n}$ if the amplitude of shear stress τ_a acting on this plane exceeds a threshold τ_a^{th}. τ_a is defined as the radius of the smallest circle circumscribing the path described by $\underline{\tau}(\underline{n},t)$ during the last loading cycle. Once again, the randomised algorithm [22] is used to determine this circle. The threshold τ_a^{th} is then supposed to be a random variable following a Weibull distribution characterised by a shape parameter m and a scale parameter τ_0. Thus, the failure probability of the slip plane can be expressed by:

$$P_{Fn} = P(\tau_a \geq \tau_a^{th}) = 1 - \exp\left[-\left(\frac{\tau_a}{\tau_0} \right)^m \right] \tag{16}$$

The normal stress effect on the fatigue strength is taken into account by considering that τ_0 depends on the normal stress amplitude $\sigma_{n,a}$ and on the mean normal stress $\sigma_{n,m}$ acting

on the slip plane of normal $\underline{n}$ (Eq. 17).

$$\tau_0 = \tau_0' \frac{1 - \gamma\sigma_{n,m}}{1 + \alpha(\sigma_{n,a}/\tau_a)} \tag{17}$$

In Eq. 17, τ_0', γ and α are material parameters.

The failure probability P_{Fg} of a grain g is supposed to correspond to the maximum failure among the failure probabilities of its slip planes (Eq. 18). This assumption constitutes the major difference with respect to the initial criterion. Indeed, the weakest-link hypothesis was used by Morel and Huyen to determined the failure probability at the grain scale P_{Fg}.

$$P_{Fg} = \max_{\underline{n} \in g} [P_{Fn}] \tag{18}$$

Finally, the weakest-link hypothesis is applied to determine the failure probability of a polycrystalline aggregate P_{Fa} which leads to the following expression:

$$1 - P_{Fa} = \prod_{g=1}^{N_g} (1 - P_{Fg}) \tag{19}$$

where N_g is the number of grain constituting the polycrystalline aggregate. The use of the weakest-link hypothesis is justified by the fact that in HCF regime, the failure is driven by the initiation and the propagation of a single crack more than the initiation and the coalescence of a large number of cracks.

3.4. Identification of the fatigue criteria parameters and predictions of the fatigue limits

For each constitutive models assigned to the grains, the parameters of the criteria are identified thanks to the results of the numerical simulation of polycrystalline aggregates loaded, at the mean fatigue limit level, in fully reversed tension and in fully reversed shear. Moreover, as the probabilistic criterion has a parameter which defined the sensitivity to the mean normal stress, the results obtained from a third loading case are needed. The loading case chosen is cyclic tension with a stress ratio $R = 0$.

The average fatigue limits of a pure copper at 10^7 cycles in cyclic symmetrical ($R = -1$) and asymmetrical ($R = 0$) tension, respectively $s_{-1} = 78MPa$ and $s_0 = 54MPa$, have been determined from experimental results by Lukàš et al. [23]. The fatigue limit in fully reversed torsion $t_{-1} = 50MPa$ has been estimated from the fatigue tests conducted by Ravilly and reported in [24].

For the integral and the critical plane-based criteria, the parameters are identified such as σ_{DV}/β_{DV} and σ_P/β_P are, in average on the 9 realisations, equal to 1 in fully reversed tension and in fully reversed shear. Regarding the probabilistic criterion, the procedure is similar excepted that the shape parameter m is imposed and two values are arbitrarily chosen (5 and 20) in order to investigate the influence of this parameter on the predictions of the criterion. The other parameters, namely τ'_0, α and γ, are identified such as P_{Fa} is, in average, equal to 50% for each of the three loading cases.

Once the parameters identified, the fatigue criteria are used to predict the fatigue strength for other loading cases. For a given loading case, the determination of the predicted average fatigue limit consists in searching the normal and shear stress amplitudes which have to be applied to the polycrystalline aggregates such as in average on the 9 realisations:

- $\sigma_{DV}/\beta_{DV} = 1$ for the critical plane criterion;
- $\sigma_P/\beta_P = 1$ for the integral criterion;
- $P_{Fa} = 50\%$ for the probabilistic criterion.

When elastic constitutive models are used, only one FE computation per loading condition is needed to determine this loading amplitude thanks to the linearity of the mechanical response. On the contrary, in cases where crystal plasticity is assigned to the grains, the search of the fatigue limit level is an iterative process requiring several FE simulations per loading condition which leads to important computation times. For that reason, the fatigue limits are predicted only for some loading cases when crystal plasticity is used.

4. Results and discussion

4.1. Effect of the constitutive models on the mesoscopic mechanical responses

The mechanical response of the polycrystalline aggregates is studied at the grain scale through the mesoscopic mechanical quantities computed from the results obtained at the last cycle of the FE simulations and for the three material behaviours assigned to the grains.

4.1.1. Comparison between macroscopic and mesoscopic mechanical responses

It has to be noted that the anisotropy of the material behaviour makes the stress-strain response of each grain to differ notably from the macroscopic response. An illustration of this fact is given in Fig.3, which represents the cyclic σ_{11}-ε_{11} (resp. σ_{12}-ε_{12}) response of each grain contained in one polycrystalline aggregate loaded in fully reversed tension (resp. fully reversed shear) with an amplitude corresponding to the experimental fatigue limit. The results obtained in the case of the cubic elasticity and in the case of the crystal plasticity in addition to the cubic elasticity are grouped respectively in Fig.3a and Fig.3b. From these figures, it can be observed that both cubic elasticity and crystal plasticity have a striking impact on the scatter of the mesoscopic stress and strain responses.

It is worth noting that the use of an anisotropic constitutive model at the grain scale results in a multiaxial stress states in the grains even in cases where a uniaxial loading is applied to the polycrystalline aggregates as it is shown in Fig.4. In this figure, the σ_{11}-σ_{22} and σ_{11}-σ_{33} responses of the grains of one polycrystalline aggregate loaded in fully reversed tension with a stress amplitude equal to the experimental fatigue limit are presented. Fig.4a corresponds to the case where cubic elasticity is used whereas Fig.4b presents the results obtained when the cubic elastic and crystal plastic model is applied to the grains. In Fig 4b, one can notice that the addition of the crystal plasticity induced non-proportional stress paths at the grain scale.

4.1.2. Distributions of the shear and normal stress amplitudes

The following analysis is focused on the mechanical quantities used in the Morel and Huyen criterion: the shear stress amplitude τ_a and the normal stress amplitude $\sigma_{n,a}$. In each subfigure of Fig.5, the response, in terms of τ_a-$\sigma_{n,a}$, of each slip plane of the nine studied configurations (3 microstructures $\times$ 3 orientations sets) is reported. The distribution, the mean value (μ) and the maximum value of each component are also given. On this figure, the results obtained with the isotropic elastic behaviour, the cubic elastic behaviour and the combination of the cubic elasticity and the crystal plasticity in the cases of fully reversed tension, fully reversed shear, combined tension-shear ($k_{12} = 0.5$, $\varphi_{12} = 0°/90°$) and biaxial tension ($k_{22} = 1$, $\varphi_{22} = 0°$) are presented. The loading amplitude applied on the aggregates corresponds to the macroscopic median fatigue limit. In the cases of fully reversed tension

and fully reversed shear, the median fatigue limits are known whereas in the other loading cases, the loading levels corresponding to the median fatigue limits are estimated with the Papadopoulos criterion.

From these results, it can be observed that, when crystal plasticity is used, the distribution of the shear stress amplitude is much less scattered in the case of combined tension-shear with $k_{12} = 0.5$ and $\varphi_{12} = 90°$ than in the other cases. Thus, this particular loading case should lead to a more homogeneous distribution of the plastic slip in the polycrystalline aggregates.

It can be stated from Fig.5 that the distributions of the considered mechanical quantities are strongly affected when the isotropic elasticity is replaced by the cubic elastic behaviour. Indeed, compared to the isotropic elastic behaviour, the cubic elasticity causes a significant increase of the maximum and the mean values of the normal stress amplitude. Conclusions about the shear stress amplitude are slightly different. Indeed, even though an increase of the maximum value of τ_a is observed, a slight decrease of its mean value is found. It should be noted that the use of cubic elasticity instead of isotropic elasticity symmetrises significantly the shear stress amplitude distributions. This leads to a decrease in the number of slip planes exhibiting high shear stress level. The trends described here for the five presented cases have also been observed for the other studied loading cases.

When compared to the cubic elastic behaviour alone, it appears that the addition of crystal plasticity only slightly affects the distributions of the two considered mechanical quantities. Indeed, its effect on the normal stress amplitude distribution is almost negligible. Furthermore, the distribution of τ_a becomes slightly more asymmetric (excepted in the case of biaxial tension) which leads to maintain the mean value while the maximum value decreases. Similar conclusions on the significant influence of the cubic elasticity compared to the crystal plasticity on the mesoscopic mechanical response were drawn by Robert et al. [8].

The moderate role of the crystal plasticity compared to the cubic elasticity can be explained in the present case by two factors. Firstly, the loading amplitudes which correspond approximately to the macroscopic median fatigue limit are close to the macroscopic yield limit so the plastic activity remains low. Secondly, the considered material has a strong anisotropic elastic behaviour. Indeed, its anisotropy coefficient, which is defined by $a = 2C_{1212}/(C_{1111} - C_{1122})$, is equal to 4.38 which is far more higher than the ones of pure

aluminium ($a \simeq 1.2$ [25]) and of pure nickel ($a \simeq 2.4$ [26]).

4.1.3. Critical slip planes orientations

The probabilistic fatigue criterion is used in order to study the most critical slip planes orientations for some loading cases. To conduct this analysis, for each grain contained in a polycrystalline aggregate, the failure probability P_{Fg} is first computed and associated to the orientation of the unit vector $\underline{n}_s$ normal to the corresponding slip plane of the considered grain. Then, each of these unit normal vectors $\underline{n}_s$ is represented by a point in Fig.6, thanks to a stereographic projection, in the plane of normal vector $\underline{e}_3$ (the reference frame is illustrated in Fig.2). The horizontal and vertical directions are respectively collinear to $\underline{e}_1$ and $\underline{e}_2$. In this figure, the colours associated to the points correspond to the magnitude of the failure probability P_{Fg}. For each loading condition studied, the failure probabilities are computed from the results of the FE models using isotropic elasticity, cubic elasticity and the combination of cubic elasticity and crystal plasticity. All results are reported in figure 6. For each constitutive model, the polycrystalline aggregates are loaded at the average fatigue limit level according to the probabilistic fatigue criterion. Only the grains having a failure probability $P_{Fg} > 10^{-5}$ are reported.

In Fig.6, it can been seen that the change of constitutive model assigned to the grains does not strongly change the pattern resulting from the projection of the most critical planes' normals. Nevertheless, the scatters observed in the values of P_{Fg} and in the orientations are increased in most cases when an anisotropic constitutive model is used. Moreover, the location, in the pole figures, of the maximal value of P_{Fg} is different than in the isotropic elastic case and depends on the realisation (microstructure geometry or orientations set).

In fully reversed tension, in the case of cubic elasticity and crystal plasticity, it can be observed that the normals of the most critical planes, i.e. the planes for which a crack initiation is most likely to occur, are inclined from 0° to 50° with respect to the loading axis. Thus, if the predictions obtained for a bulk material are similar to those obtained for grains located at a free surface then the angle between the intersection of the crack planes with the surface and the loading axis will range from 40° to 90°. These remarks are in accordance with experimental observations made from low-cycle fatigue tests on an austenitic stainless steel [27].

4.2. Predictions of the fatigue criteria

Noting the differences between the macroscopic and the mesoscopic responses, one can wonder how fatigue criteria based on macroscopic mechanical quantities can predict rather accurately the fatigue limits. Even fatigue criteria using a mesoscopic approach are able to provide satisfactory predictions (see for instance [2] and [4]) despite the frequent use of simplifying assumptions. Among these hypotheses usually postulated, one can cite the omission of the elastic anisotropy and the Lin-Taylor homogenisation assumption which is invalidated by the present study (see Fig.3).

To provide some answers to this question, the predictions of the fatigue criteria described in section 3 are determined for each constitutive model used at the grain scale and are compared to each other. The fatigue limits predicted by the criteria, when an isotropic elastic model is used, will serve as references because in that particular case, the mesoscopic stress tensor $\langle \boldsymbol{\sigma} \rangle_g$ correspond to the macroscopic stress tensor $\boldsymbol{\Sigma}$. Thus, for this constitutive model, the predictions provided by the criteria will be similar to those given by the original criteria ([1], [2] and [4]).

Besides, in this section, the experimental trends observed in multiaxial high cycle fatigue for metallic materials are summarised. Then, the predictions obtained from the three fatigue criteria are presented and compared to these trends. In order to make a reasonable comparison between the experimental and the predicted fatigue limits, the experimental data selected here concern metallic materials which have a ratio s_{-1}/t_{-1} close to the one of the studied copper and the fatigue limits are normalised.

4.2.1. Combined tension and shear

According to the experimental data found in the literature, it appears that no clear trend can be observed regarding the effect of the phase shift on the fatigue strength of various metallic materials subjected to tensile-torsion loads. Indeed, for a given biaxiality ratio k_{12}, in some cases an increase in phase shift (for $\varphi_{12} \in [0°; 90°]$) has a beneficial influence on the fatigue strength [16, 17] while in other cases, it can have a negligible [18] or even a detrimental [17, 19] effect. These experimental results, in addition to the fatigue limits determined by Mielke [20], are reported in Fig.7 which represents the normalised average fatigue limits for combined tension and shear in cases where $\varphi_{12} = 0°$, $\varphi_{12} = 90°$ and $k_{12} = 0.5$.

In this figure, the fatigue limits predicted by the three fatigue criteria, for the two elastic constitutive models studied, are also presented. The fatigue limits determined when an isotropic elastic model is assigned to the grains (Fig.7a) are not particularly surprising. Indeed, thanks to a sufficiently large number of grains considered, the predictions provides by the critical plane-based criterion and the integral criterion were found to be the same as the ones obtained respectively from the Dang Van and the Papadopoulos criteria and the fatigue limits provided by the probabilistic fatigue criterion are only slightly different from those given by the Morel and Huyen criterion [4]. These differences are mainly due to the change made on the initial criterion.

According to the critical plane-based criterion, an increase of the phase difference φ_{12} (for $0°$ to $90°$) leads to a beneficial effect on the fatigue strength while the integral criterion predicts that the phase shift does not affect the fatigue limit of the material loaded in combined tension and shear. In the case of in-phase tension-shear, the probabilistic criterion gives predictions similar to those of the integral criterion and slightly more optimistic than those of the critical plane criterion. Besides, in cases of high phase differences ($\varphi_{12} \in [45°; 90°]$), fatigue limits estimated by the probabilistic fatigue criterion lies between the ones predicted by the Papadopoulos and Dang Van criteria. It is worth noting that the shape parameter m, in the considered range of values, does not strongly affect the average fatigue limits predicted by the probabilistic criterion. The maximum difference encountered, occuring for $\varphi_{12} = 90°$ and $k = 1$, results in an increase of about 4% of the predicted fatigue limits for m ranging from 20 to 5.

From the results presented in Fig.7a, it appears that the fatigue limits provided by all the considered criteria are in good agreement with experimental data for in-phase tension and shear fully reversed loadings. On the contrary, in the case of high phase shift, the critical plane-based criterion mostly overestimates the fatigue strength while the integral criterion generally provides conservative predictions. At last, the probabilistic criterion seems to be a good alternative to the integral criterion only for materials showing a significant fatigue strength improvement due to phase shift.

Comparing the results reported in Figs. 7a and 7b, it appears that the average fatigue limits predicted by a given criterion with the cubic elastic model are surprisingly close to those estimated by the same criterion with the isotropic elastic model. Indeed, when $\varphi_{12} = 0°$, the

maximum difference observed, relative to the case of the isotropic elasticity, is lower than 8% for the critical plane criterion and 1% for the two other criteria. In the case where $\varphi_{12} = 90°$, differences between fatigue limits predicted for the two constitutive models are lower than 2% for the critical plane criterion, 1% for the integral criterion and 5% for the probabilistic criterion regardless of the m value considered.

The fatigue limits have also been estimated by the criteria when crystal plasticity was used in the FE models for some loading cases, namely ($k_{12} = 0.5, \varphi_{12} = 0°$) and ($k_{12} = 0.5, \varphi_{12} = 90°$). These predictions are summarised in Fig.8 together with those determined in the case where only cubic elasticity was assigned to the grains. It can be observed that the addition of the crystal plasticity does not significantly affect the predictions whatever the criterion. Indeed, differences between predictions are lower than 1% excepted for the critical plane-based criterion where a difference of approximately 3% is observed when $k_{12} = 0.5$ and $\varphi_{12} = 90°$.

Thus, despite the fact that the distribution of the mesoscopic mechanical quantities are misestimated (especially concerning the normal stress acting on the slip planes) when the hypothesis that grains have an isotropic elastic behaviour is made, the three studied criteria provide almost identical predictions to those obtained from FE models using cubic elasticity or combination of cubic elasticity and crystal plasticity, at least for the cases of combined tension and shear.

4.2.2. Biaxial tension

In the case of biaxial tension, only a small number of experimental results has been reported. In this context, the conclusions on possible experimental trends have to be taken with caution. From the fatigue tests conducted by Rotvel [21] and Koutiri [5], whose results are presented in Fig.9, it can be observed that if no phase shift is applied, the increase of the biaxiality ratio (for $k_{22} \in [0; 1]$) has a negligible effect on the fatigue limit defined by $\Sigma_{11,a}$. In the case of a phase shift $\varphi_{22} = 180°$, a decrease of the fatigue limit is observed for high biaxiality ratio values ($k_{22} = 0.8$ and $k_{22} = 0.83$). This latter finding is not surprising given that these loading cases are close to the pure shear stress state (i.e. $k_{22} = 1.0$ and $\varphi_{22} = 180°$) and that the crystallographic texture is isotropic.

The fatigue limits predicted by each criterion using isotropic elasticity and cubic elasticity are shown respectively in Figs. 9a and 9b. The same remarks as in the previous subsection

can be made about the concordance of the predictions obtained from the initial criteria and from the criteria applied to the FE results in which isotropic elasticity is used. For this constitutive model, it can be observed that the critical plane criterion predicts systematically a detrimental effect on the fatigue strength when the biaxiality ratio k_{22} increases from 0 to 1, whatever the phase shift φ_{22} is. As for the two other criteria, when $\varphi_{22} \geq 90°$, a decrease of the fatigue limit is also predicted for an increase of k_{22}. However, in the case where $\varphi_{22} < 90°$ a slight improvement of the fatigue limit is first encountered with the increase of the biaxiality ratio up to approximately 0.5 then a slight decrease is noted for k_{22} ranging from 0.5 to 1. Moreover the shape parameter m, once again, does not affect significantly the average fatigue limits predicted by the probabilistic criterion for the two considered values. The maximum difference encountered does not exceed 3% for m ranging from 5 to 20.

According to the predictions obtained for $\varphi_{22} = 0°$, it appears that the integral and the probabilistic criteria are the most likely to account for the experimental trends while the critical plane criterion provide conservative fatigue limits. Unfortunately, the lack of experimental data, in the case of fully reversed biaxial tension, does not afford the possibility to draw a definitive conclusion about the predictive accuracy of the criteria.

Unlike the case of combined tension and shear, the comparison between the predicted fatigue limits illustrated in figures 9a and 9b reveals a noteworthy sensitivity of the predictions provided by some criteria with respect to the constitutive model assigned to the grains, especially for in-phase loading cases. Indeed, the differences encountered between the predicted fatigue limits obtained in the cases of isotropic elasticity and cubic elasticity can reach 15% for the critical plane criterion over the whole range of biaxiality ratio and respectively 5% and 10% for the probabilistic criterion for $m = 5$ and $m = 20$. Nevertheless, the integral criterion remains unchanged when cubic elasticity replaces isotropic elasticity. Indeed, the differences between the predictions provided by this criterion for the two constitutive models never exceed 1%.

The fatigue limits have been determined by the criteria when crystal plasticity was used in the FE models for some loading cases for which significant differences between the predictions obtained with the isotropic elasticity and the cubic elasticity were found, namely $(k_{22} = 0.5, \varphi_{22} = 0°)$, $(k_{22} = 1, \varphi_{22} = 0°)$ and $(k_{22} = 1, \varphi_{22} = 90°)$. These predictions and those determined in the case where only cubic elasticity was assigned to the grains are re-

ported in Fig.10. Once again, it can be stated that the addition of the crystal plasticity affects only slightly the predictions. Indeed, differences between predictions are lower than 1% for the integral criterion, 2% for the probabilistic criterion and 3% for the critical plane criterion.

From these results, it can be observed that the integral criterion provides predictions which are almost unaffected by the constitutive model used at the grain scale. This is due to the fact this criterion used averaged mechanical quantities over the entire aggregate. On the contrary, the critical plane criterion that uses the stress state of the most stressed slip plane in the aggregate is the criterion whose predicted fatigue limits are the more affected by the change of constitutive model. At last, the predictions given by the probabilistic criterion are more or less sensitive to this change depending on the value of m. The higher the shape parameter, the more affected are the predictions. This is due to the fact that the increase of the shape parameter leads to a decrease of the variance of the Weibull distribution, thereby emphasising the contribution of the most stressed grains on the failure probability of the aggregate and making negligible the one of a larger number of grains. In other words, for high m values, only one or a few grains contribute effectively to the failure, like in the case of the critical plane criterion, whereas for low m values, all the grains in the aggregate are taken into account to evaluate the risk of failure, like the integral criterion.

5. Conclusion

The cyclic mechanical responses of polycrystalline aggregates, obtained from finite element simulations, have been analysed for various loading conditions. It was reminded that the mesoscopic responses, in terms of stress or strain, are scattered and differ significantly from the macroscopic response of the polycrystalline aggregate. Moreover, the anisotropy of the grains' behaviour leads to a multiaxial response even when an uniaxial loading is applied to the polycrystal. Furthermore, the introduction of the crystal plasticity in the constitutive model of the grains induced a non-proportionality between the components of the stress tensor during the loading cycle. At last, the influence of each source of anisotropy (elastic and plastic) on the distributions of shear and normal stresses have been discussed. It has been highlighted that the cubic elasticity, unlike the crystal plasticity, significantly affects these distributions for a wide variety of loading cases. Two factors may explain these results: the

strong anisotropic elastic behaviour of the copper single crystal and the fact that the loading amplitudes in high cycle fatigue leads to moderate plastic strains.

The predictions obtained from three different criteria using the results of the FE computations are then studied. It appears that they are generally not very sensitive to the constitutive model assigned to the grains, for the loading cases studied, despite remarkable differences between the mesoscopic and macroscopic responses. The most notable differences are encountered for biaxial tension loading with the critical plane criterion and the probabilistic criterion (when the shape parameter is high). It follows that if these criteria provide good predictions with a complex modelling, they are able to satisfactorily estimate the fatigue limits with a simple modelling. Moreover, it has been observed, from the comparison between experimental trends and numerical predictions, that the integral and the probabilistic fatigue criteria reflect quite well the effects of biaxiality and phase shift on the fatigue strength for the considered loading conditions. However, these conclusions should be taken with caution. Indeed, some aspects have been omitted (for instance, the free surface, microstructural heterogeneities) or simplified (the microstructures are modelled with 2-dimensional polycrystalline aggregates and a generalised plane strain hypothesis is used) in the modelling and several loading conditions have not yet been studied. Besides, another issue that has not been discussed here is the opportunity offered by the polycrystalline aggregates simulations to study the microstructural heterogeneities (micro-notches, precipitates, pores...) effect on the HCF behaviour which could provide deeper understanding of the experimental trends.

[1] K. Dang-Van, Macro-micro approach in high-cycle multiaxial fatigue, in: ASTM Special Technical Publication, 1993, pp. 120–130.

[2] I. Papadopoulos, A new criterion of fatigue strength for out-of-phase bending and torsion of hard metals, International Journal of Fatigue 16 (6) (1994) 377–384.

[3] V. Monchiet, E. Charkaluk, D. Kondo, Plasticity-damage based micromechanical modelling in high cycle fatigue, Comptes Rendus Mécanique 334 (2) (2006) 129–136.

[4] F. Morel, N. Huyen, Plasticity and damage heterogeneity in fatigue, Theoretical and Applied Fracture Mechanics 49 (1) (2008) 98–127.

[5] I. Koutiri, Effet des fortes contraintes hydrostatiques sur la tenue en fatigue des matériaux métalliques, Ph.D. thesis, Arts et Métiers ParisTech (2011).

[6] V. Bennett, D. McDowell, Polycrystal orientation distribution effects on microslip in high cycle fatigue, International Journal of Fatigue 25 (1) (2003) 27–39.

[7] Y. Guilhem, S. Basseville, F. Curtit, J.-M. Stéphan, G. Cailletaud, Investigation of the effect of grain clusters on fatigue crack initiation in polycrystals, International Journal of Fatigue 32 (11) (2010) 1748–1763.

[8] C. Robert, N. Saintier, T. Palin-Luc, F. Morel, Micro-mechanical modelling of high cycle fatigue behaviour of metals under multiaxial loads, Mechanics of Materials 55 (2012) 112–129.

[9] X. Fang, W. Yan, H. Gao, Z. Yue, J. Liu, F. Wang, Finite element simulation of surface deformation of polycrystal with a rough surface under repeated load , Finite Elements in Analysis and Design 60 (2012) 64–71.

[10] A. Le Pécheur, F. Curtit, M. Clavel, J.M. Stephan, C. Rey and Ph. Bompard, Polycrystal modelling of fatigue: Pre-hardening and surface roughness effects on damage initiation for 304L stainless steel, International Journal of Fatigue 45 (2012) 48–60.

[11] L. Méric, G. Cailletaud, M. Gaspérini, F.E. calculations of copper bicrystal specimens submitted to tension-compression tests, Acta Metallurgica et Materialia 42 (3) (1994) 921–935.

[12] P. Franciosi, Etude théorique et expérimentale du comportement élastoplastique des monocristaux métalliques se déformant par glissement : modélisation pour un chargement complexe quasi statique, Ph.D. thesis, Université Paris Nord - Paris 13 (1984).

[13] C. Gérard, F. NGuyen, N. Osipov, G. Cailletaud, M. Bornert, D. Caldemaison, Comparison of experimental results and finite element simulation of strain localization scheme under cyclic loading, Computational Materials Science 46 (3) (2009) 755–760.

[14] C. Geuzaine, J. Remacle, Gmsh: A 3-d finite element mesh generator with built-in pre-and post-processing facilities, International Journal for Numerical Methods in Engineering 79 (11) (2009) 1309–1331.

[15] J. Besson, R. Leriche, R. Foerch, G. Cailletaud, Object-oriented programming applied to the finite element method part II. application to material behaviors, Revue Européenne des Éléments 7 (5) (1998) 567–588.

[16] T. Nishihara, M. Kawamoto, The strength of metals under combined alternating bending and torsion with phase difference, Memoirs of the College of Engineering, Kyoto Imperial University 11 (1945) 85–112.

[17] S. Lasserre, C. Froustey, Multiaxial fatigue of steel–testing out of phase and in blocks: validity and applicability of some criteria, International Journal of Fatigue 14 (2) (1992) 113–120.

[18] R. Heidenreich, I. Richter, H. Zenner, Schubspannungsintensitätshypothese–weitere experimentelle und theoretische untersuchungen, Konstruktion 36 (3) (1984) 99–104.

[19] W. Lempp, Festigkeitsverhalten von stählen bei mehrachsiger dauerschwingbeanspruchung durch normalspannungen mit überlagerten phasengleichen und phasenverschobenen schubspannungen, Ph.D. thesis, TU Stuttgart (1977).

[20] S. Mielke, Festigkeitsverhalten metallischer werkstoffe unter zweiachsiger schwingender bean-spruchung mit verschiedenen spannungszveitverlaufen, Ph.D. thesis, TH Aachen (1980).

[21] F. Rotvel, Biaxial fatigue tests with zero mean stresses using tubular specimens, International Journal of Mechanical Sciences 12 (7) (1970) 597–613.

[22] A. Bernasconi, I. Papadopoulos, Efficiency of algorithms for shear stress amplitude calculation in critical plane class fatigue criteria, Computational Materials Science 34 (4) (2005) 355–368.

[23] P. Lukàš, L. Kunz, Effect of mean stress on cyclic stress-strain response and high cycle fatigue life, International Journal of Fatigue 11 (1) (1989) 55–58.

[24] A. M. Freudenthal, E. J. Gumbel, On the statistical interpretation of fatigue tests, Proceedings of the Royal Society of London. Series A. Mathematical and Physical Sciences 216 (1126) (1953) 309–332.

[25] S. Balasubramanian, L. Anand, Elasto-viscoplastic constitutive equations for polycrystalline fcc materials at low homologous temperatures, Journal of the Mechanics and Physics of Solids 50 (1) (2002) 101–126.

[26] G. Alers, J. Neighbours, H. Sato, Temperature dependent magnetic contributions to the high field elastic constants of nickel and an fe-ni alloy, Journal of Physics and Chemistry of Solids 13 (12) (1960) 40–55.

[27] P. Mu, V. Aubin, I. Alvarez-Armas, A. Armas, Influence of the crystalline orientations on microcrack initiation in low-cycle fatigue, Materials Science and Engineering: A 573 (2013) 45–53.

List of Figures

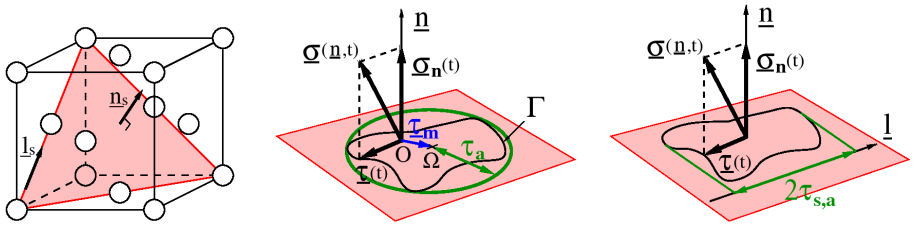

(a) (b)

Figure 1: Representation of some mechanical quantities and vectors in (a) a FCC unit cell and (b) a slip plane.

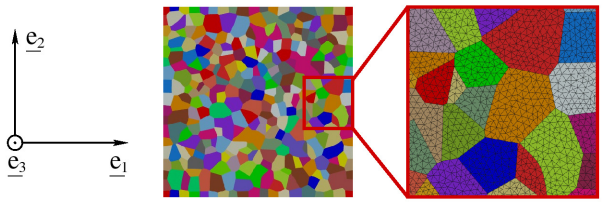

Figure 2: Geometry and detailled view of the mesh of a periodic 2-dimensional polycrystalline aggregate with 300 grains and in average 100 elements per grain.

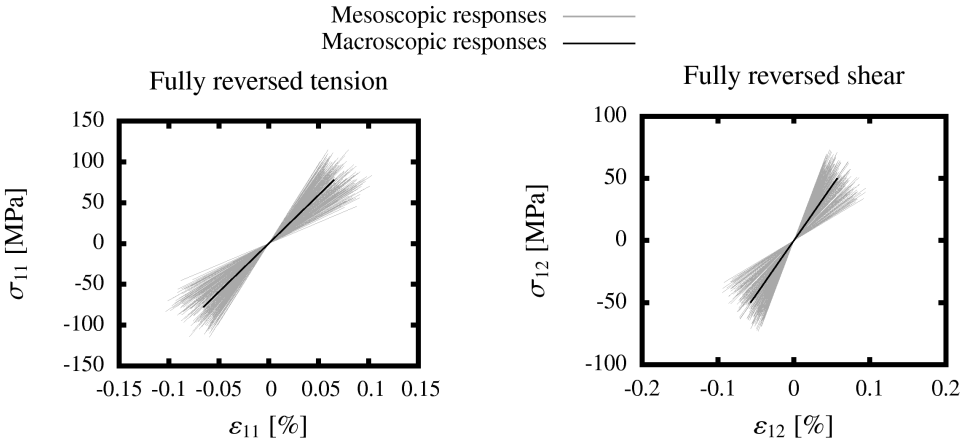

(a) Cubic elasticity

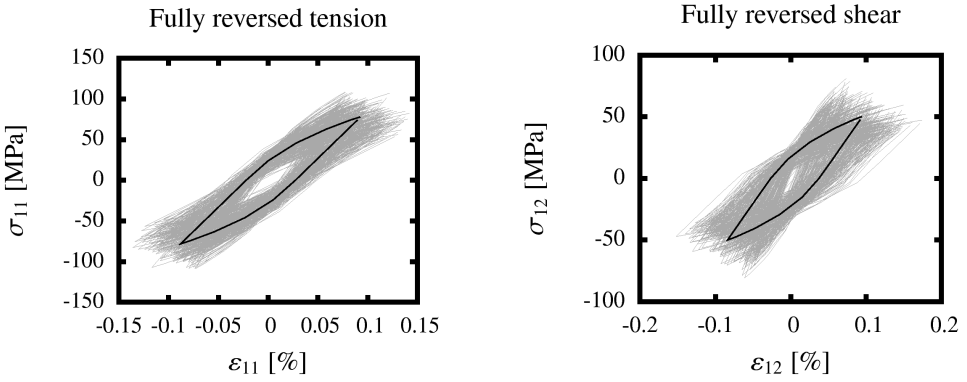

(b) Cubic elasticity and crystal plasticity

Figure 3: Comparison between the macroscopic and the mesoscopic stress-strain responses of one polycrystalline aggregate loaded at the fatigue limit level in fully reversed tension and in fully reversed shear for: (a) a cubic elastic model and (b) a cubic elastic and crystal plastic model assigned to the grains.

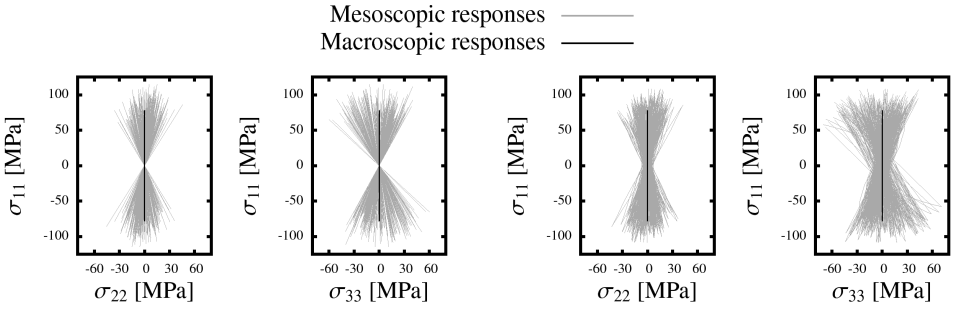

(a) Cubic elasticity (b) Cubic elasticity and crystal plasticity

Figure 4: Comparison between the macroscopic and the mesoscopic σ_{11}-σ_{22} and σ_{11}-σ_{33} responses of one polycrystalline aggregate loaded at the fatigue limit level in fully reversed tension for: (a) a cubic elasticity model and (b) a cubic elasticity and crystal plasticity model assigned to the grains.

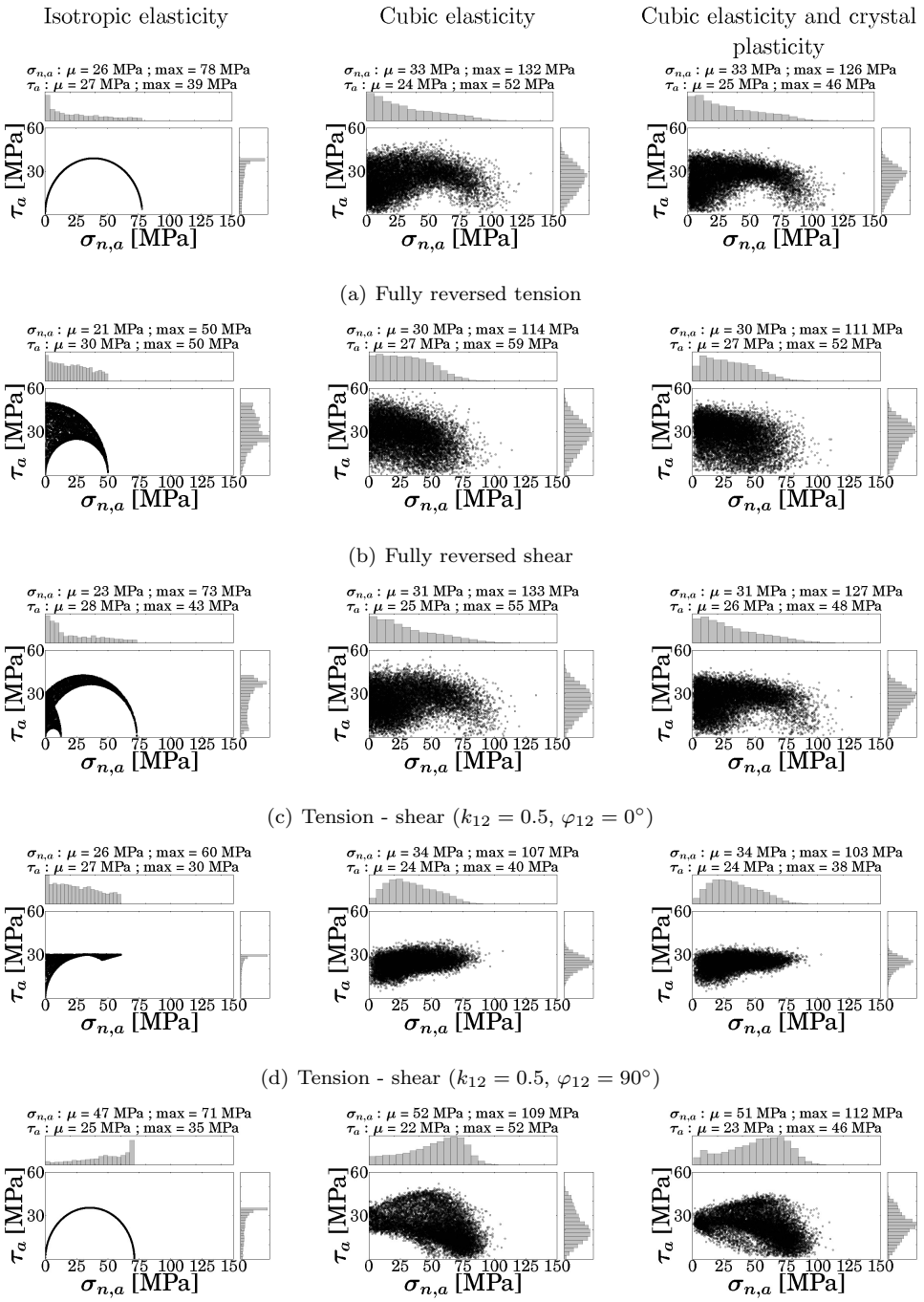

(a) Fully reversed tension

(b) Fully reversed shear

(c) Tension - shear ($k_{12} = 0.5$, $\varphi_{12} = 0°$)

(d) Tension - shear ($k_{12} = 0.5$, $\varphi_{12} = 90°$)

(e) Biaxial tension ($k_{22} = 1$, $\varphi_{22} = 0°$)

Figure 5: Mechanical responses, in terms of τ_a-$\sigma_{n,a}$, of each slip planes obtained from the FE simulations of polycrystalline aggregates for different loading cases.

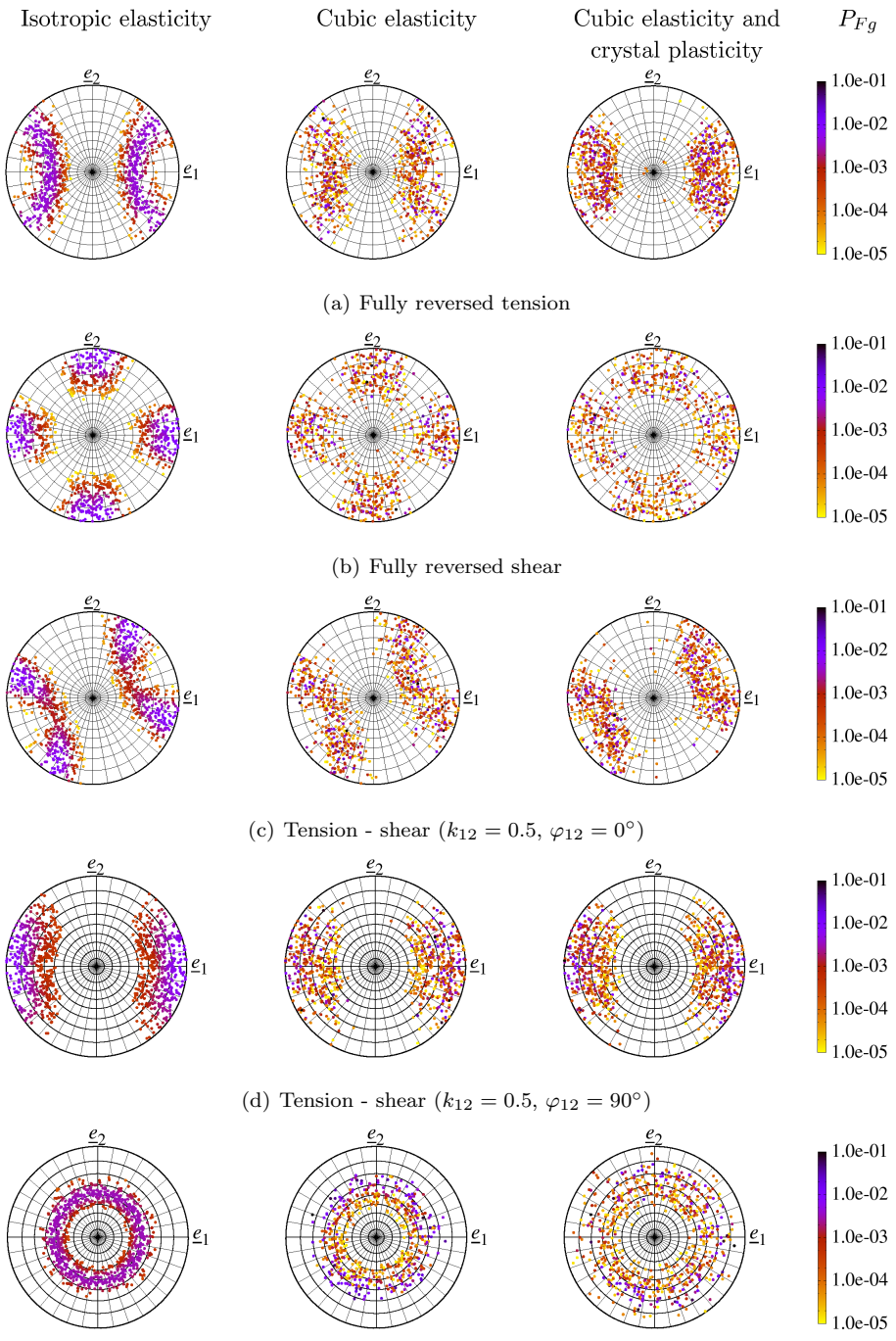

(a) Fully reversed tension

(b) Fully reversed shear

(c) Tension - shear ($k_{12} = 0.5$, $\varphi_{12} = 0°$)

(d) Tension - shear ($k_{12} = 0.5$, $\varphi_{12} = 90°$)

(e) Biaxial tension ($k_{22} = 1$, $\varphi_{22} = 0°$)

Figure 6: Stereographic projection, in the plane of normal $\underline{e}_3$, of the unit vector normal to the most critical slip plane of each grain and associated failure probability P_{Fg}.

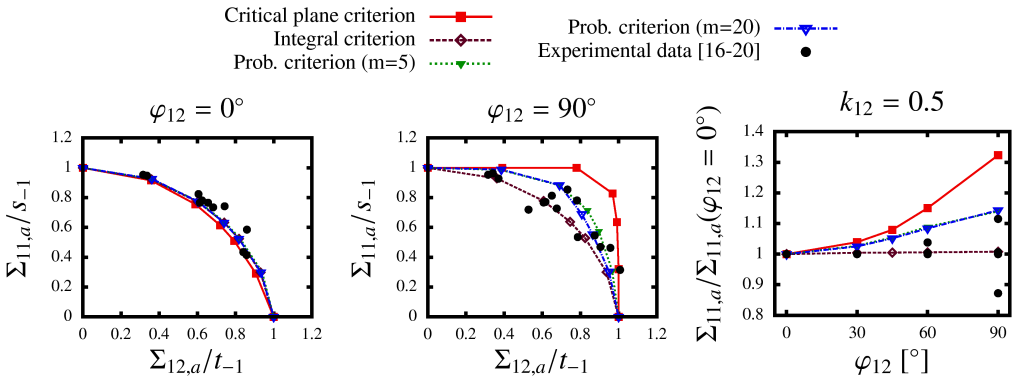

(a) Isotropic elasticity

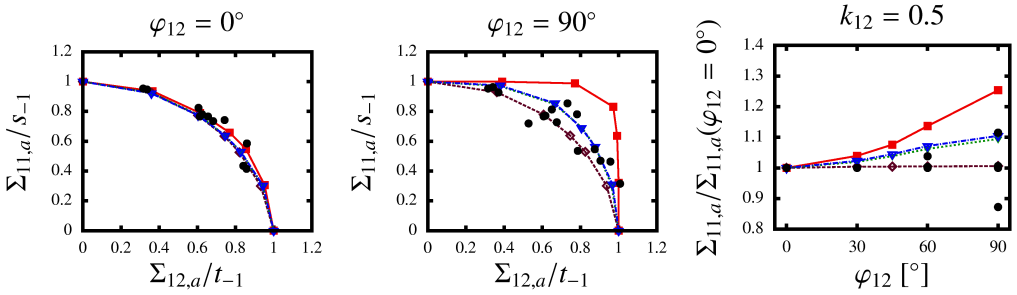

(b) Cubic elasticity

Figure 7: Predictions of the fatigue criteria in combined tension and shear for each elastic constitutive models and experimental fatigue limits of different metallic materials.

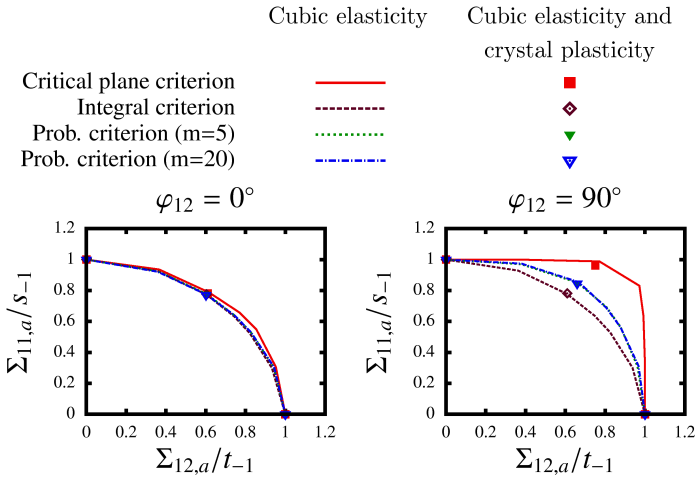

Figure 8: Comparison between the predictions of the fatigue criteria in combined tension and shear obtained with cubic elasticity and with crystal plasticity in addition to cubic elasticity.

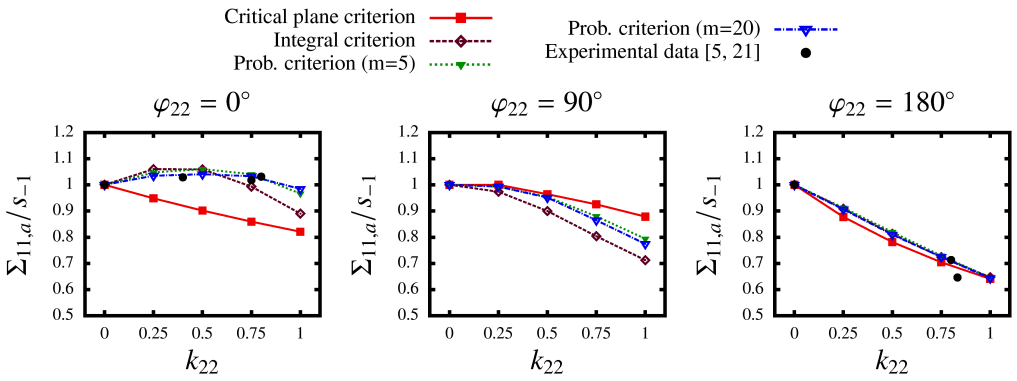

(a) Isotropic elasticity

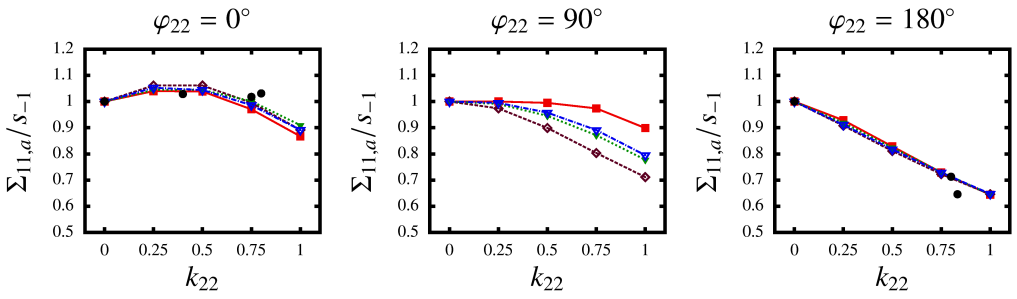

(b) Cubic elasticity

Figure 9: Predictions of the fatigue criteria in biaxial tension for each elastic constitutive models and experimental fatigue limits of different metallic materials.

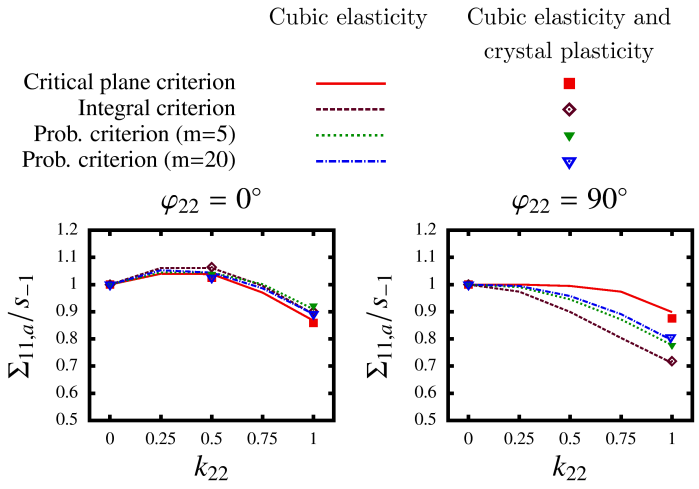

Figure 10: Comparison between the predictions of the fatigue criteria in biaxial tension obtained with cubic elasticity and with crystal plasticity in addition to cubic elasticity.